Indian Journal of
Applied Radiology

Open Science Publications

Volume 7, Issue 1 - 2021

www.opensciencepublications.com

A Comprehensive Evaluation of High-Resolution Computed Tomography (HRCT) Imaging Patterns in COVID-19 Pneumonia According to the Time Course of the Disease and Across Different Age Groups in Indian Population

Research Article

Ramesh Parate[1], Maherafsha Hundekari[1]*, Aarti Anand[1], Tilottama Parate[2] and Farhan Ansari[3]

[1]*Department of Radiology, Government Medical College Nagpur, India*

[2]*Department of Medicine, Indira Gandhi Government Medical College, Nagpur, India*

[3]*Department of Neurology, NIMHANS, Bangalore, India*

***Corresponding author:** Dr. Maherafsha Hundekari, Junior Resident, Department of Radiology,Government Medical College Nagpur,Hanuman Nagar-440024, Nagpur, India, Tel: 7798100399 E-mail: maherafsha@gmail.com

Article Information: **Submission: 22/02/2021; Accepted: 27/05/2021; Published: 31/05/2021**

Abstract

Objectives: To elucidate the chest HRCT imaging manifestations in coronavirus (COVID-19) infected Indian patients, study and compare the patterns identified during time course and among differently aged patients.

Materials and Methods: A retrospective observational study of 500 laboratory-confirmed SARS-CoV-2 infected patients was performed. The patients were categorized into 3 groups based on the time interval between onset of symptom and HRCT imaging and according to their age. The distribution, patterns, and extent of lung abnormalities were recorded.

Results: A predominant peripheral distribution of the abnormalities was observed as in 262/390 patients (67.2%). The Mean CT score of the right lower lobe (2.06 ± 1.13) and left lower lobe (2.01 ± 1.128) were significantly greater than other lung lobes (P-value < 0.001). Overall, most commonly observed pattern on imaging was crazy-paving pattern observed in 329/390 patients (84.4%). In the early phase of the disease (0-7 days), predominant patterns were crazy-paving (90.7%) and GGO with consolidation (50.4%). The consolidation pattern and the vacuolar sign showed a significant rise during advanced phase of the disease (8-14 days of symptom onset) and eventually decreased during the absorption phase (> 14 days after symptom onset). The reticular pattern, subpleural line sign were the dominant patterns observed during the absorption phase. The Mean total CT severity score (9.79 ± 4.79) was greatest for group C patients: age ≥ 45 years. (P-value < 0.001). GGO with consolidations was more common in group B (25-44 years) and C, whereas GGO plus reticulations and reticular pattern were more common in group C (P-value < 0.001).

Conclusion: HRCT features of COVID-19 pneumonia vary according to the disease course and the patient's age. Crazy-paving pattern is dominant during the early phase and repairing signs during the absorption phase. The extent and pattern of involvement are more severe in the elderly population.

Keywords: COVID- 19; Coronavirus disease 2019; SARS- CoV-2; Severe acute respiratory syndrome coronavirus 2; CT, Computed Tomography; HRCT, High resolution computed tomography; RT-PCR, Reversetranscriptase-polymerase chain reaction

ISSN: 2581-3919

Introduction

The outbreak of COVID- 19 originated in Wuhan, China, began in December 2019, and has been continuing since then. As of 21st November 2020, more than 56,982,476 confirmed SARS- CoV-2 cases along with 1,361,847 deaths have been reported globally by the World Health Organization (WHO) [1]. Amongst these, more than 9 million cases have been reported in India [2]. At present confirmation of COVID -19 infection is done by a specific viral nucleic acid assay using reverse transcription-polymerase chain reaction (RT-PCR) on sputum, nasopharyngeal/oropharyngeal swabs and other specimens [3]. However, as per the recent literature, some patients with COVID-19 infections might show initial negative nucleic acid assay results [4]. The various reasons for a negative test could be insufficient cellular material for detection and improper extraction of nucleic acid from clinical materials [5]. Therefore Chest HRCT has higher sensitivity for the diagnosis of COVID- 19 pneumonia and presently HRCT has been used as one of the most important tools for a comprehensive evaluation and follow-up especially in epidemic areas [6].

In this study, we analyzed the HRCT lung manifestations in 500 infected patients and compared the HRCT patterns identified during the disease course and among differently aged patients.

Materials and Methods

Study Population and Design

This was a retrospective observational study approved by the ethical committee of our institute and the requirement of written informed consent was waived. It was conducted between August 15 to October 15, 2020, in our dedicated Covid hospital. Symptomatic COVID-19 infected patients were screened using the following criteria.

The inclusion criteria:

a. At least one positive RT-PCR for SARS- CoV-2 obtained with nasopharyngeal/oropharyngeal swabs.

b. At least one HRCT scan done per patient as and when requisition received from the clinicians.

The exclusion criteria:

a. Patients with RT-PCR test negative results.

b. Asymptomatic patients.

c. Technical errors within the HRCT scan.

d. Antenatal patients.

Thus, about 500 patients were included in the study. 308/500 (61.6%) were male; mean age - 43.25 years, range: 17-87 years and 192/500 (38.4%) were female; mean age - 40.76 years; range: 11-91 years. Based on age distribution: Group A: < 25 years, n= 46 (9.2%); Group B: 25-44 years, n= 236 (47.2%); Group C: ≥45 years, n= 218 (43.6%). The clinical, demographic and imaging data of all the patients were recorded.

Sub-stratification of the patients: The patients were clustered into 3 groups based on the number of days between the onset of the symptoms and the HRCT scan (course of the disease):

a. The early phase: 0- 7 days after the symptom onset.

b. The advanced phase: 8-14 days after the symptom onset.

c. The absorption phase: > 14 days after the symptom onset.

HRCT acquisition protocol: All HRCT scans were performed on a 128 slice SIEMENS CT scanner. Patients were examined in supine position and image acquired during a single inspiratory breath-hold. The scanning range extended from the apex of lung up to the adrenal glands. Following were the scanning parameters: X-ray Tube parameters- 140 KVp; 234mAs; rotation time - 0.5 s; pitch - 1.0; section thickness- 5mm; intersection space- 5 mm; additional reconstruction using the B80f ultra-sharp kernel and a slice thickness of 1 mm. Lung window setting was with a window level of -600 Hounsfield units (HU) and window width of 1500 HU. Appropriate infection and control measures were implemented.

HRCT image analysis: Two senior radiologists with 10-15 years of experience in thoracic radiology evaluated the scanned images on the console using multiplanar reconstruction tools. The patterns observed were classified into 3 major categories: lung, bronchial and pleural changes. These categories were further classified into the following subcategories:

Lung changes [7].

a. GGO- Ground glass opacities: increased attenuation without obscuration of the underlying vessels.

b. Consolidation: Homogenous increased intensity of lung parenchyma with obscuration of underlying vessels.

c. Crazy-paving pattern: GGO with an interlobular and intralobular septal thickening.

d. Reticular pattern: a disordered arrangement of coarse linear or curvilinear opacities.

e. GGO with Consolidation.

f. GGO plus Reticulations.

g. Vacuolar sign: A transparent vacuole like a shadow of < 5 mm in length observed within the lesion.

h. Halo sign: area of consolidation surrounded by GGO.

i. Reverse halo sign: area of GGO surrounded by consolidation

j. Microvascular dilation sign: dilated small vessels within the lesion.

k. Subpleural line: an arc-shaped linear shadow 2-5 cm in length appearing parallel to the chest wall.

l. Subpleural transparent line: a thin transparent line lying between the lesions and the visceral pleura.

Bronchial changes:

a. Air bronchogram: an air-filled image of bronchus in lung lesions.

b. Bronchiectasis.

Citation: Parate R, Hundekari M, Anand A, Parate T, Ansari F. A Comprehensive Evaluation of High-Resolution Computed Tomography (HRCT) Imaging Patterns in COVID-19 Pneumonia According to the Time Course of the Disease and Across Different Age Groups in Indian Population. Indian J Appl Radiol. 2021;7(1): 162.

C. Pleural changes:

a. Pleural thickening.

b. Pleural retraction: lesions pulling off the visceral pleura.

c. Pleural effusion.

d. Miscellaneous changes: Mediastinal lymphadenopathy, cavitation,calcifications,tree-in-budappearance(centrilobular nodules with a linear branching pattern).

The horizontal distribution of pulmonary lesion was noted as peripheral: involving mainly the peripheral one-third of the lung or central plus peripheral. The area of involvement was categorized as predominant anterior or posterior involvement (the area before or after the vertical line of the midpoint of the diaphragm in the sagittal position respectively). The number of lesions was noted as single or multiple (>1) lesions, the size of the lesion was accounted as: < 1 cm, 1-3 cm, and >3 cm.

A semi-quantitative CT severity scoring was used to evaluate the extent of lung involvement and was recorded for each of the 5 lobes based on anatomic involvement, as follows: 0, no involvement; 1, <5% involvement; 2, 5-25% involvement; 3, 26-50% involvement; 4, 51-75% involvement; and 5, >75% involvement. The total CT score was the sum of each lobar score: 0 to 25 [8].

Statistical analysis

Statistical analyses were performed using SPSS version 19.0. Continuous variables were expressed as Mean ± Standard Deviation, Numerical data were expressed as a percentage (%) of the total. The incidence of various HRCT characteristics, lesion distribution, predominant lung area involved was expressed as frequency (%) and compared using the Pearson Chi-Square test between the early, advanced and absorption stage as well as between the age groups. We used one-way ANOVA analysis of variance (post hoc multiple comparisons) to do pairwise comparisons for CT severity score as well as for the patterns found among the age groups. The difference was statistically significant with a P-value < 0.05.

Results

Demographic and clinical findings:

Table 1 summarizes demographic and clinical data.

HRCT findings: Out of 500 patients, parenchymal abnormalities were observed in 390 (78%) cases, while 110 (22%) cases had a normal scan. A significantly predominant peripheral distribution of the abnormalities was observed in 262/390 patients (67.2%), while central plus peripheral involvement was seen in 128/390 cases (32.8%) (P-value <0.001). A higher frequency of predominant posterior involvement (311/390) of the lung area compared to the predominant anterior involvement (79/390) was noted (P-value<0.001) (Fig 1). The mean CT score of the right lung was 4.74 ± 2.89, higher than the left lung (3.55 ± 2.05) (P-value<0.001). Among the lobes, the mean CT score of right lower lobe and left lower lobe were 2.06 ± 1.13 and 2.01 ± 1.128, significantly greater than the other lobes (P-value < 0.001), however, not much difference was noted between the scores of right lower lobe and left lower lobe (P-value=0.154) (Table 2).

Table 3 shows the detailed evaluation of various HRCT characteristics. The most common parenchymal abnormality was the crazy-paving pattern observed in 329/390 cases (84.4%). Other common patterns observed were pure GGO (60/390;15.4%); Consolidation (84/390;21.5%); GGO with consolidation (135/390;34.6%); GGO plus reticulations (176/390;45.1%); Reticular pattern (137/390;35.1%) and micro vascular dilation sign

Table 1: Demographic, clinical profile of the patients with COVID-19 infection.

Characteristic	Number (%) of patients (n = 500)
Sex	
Male	308 (61.6)
Female	192 (38.4)
Age Groups	
A (< 25 years)	46 (9.2)
B (25-44 years)	236 (47.2)
C (> 45 years)	218 (43.6)
Symptoms	
Fever	440 (88)
Sore throat	312 (62.4)
Dry cough	177 (35.4)
Myalgia	260 (52)
Dyspnea	160 (32)
Diarrhea	36 (7.2)
Accompanying condition/disease	
Hypertension	53 (10.6)
Diabetes	44 (8.8)
Chronic Kidney Disease	20 (4)
Cardiac Abnormalities	10 (2)

Table 2: Distribution and CT severity score for parenchymal abnormalities in 390 patients with COVID-19 pneumonia.

	No. (%) of Patients	CT score, Mean ± SD	P-value
Lesion Distribution			
Peripheral	262 (67.2)		<0.001*
Central + Peripheral	128 (32.8)		
Lung Area			
Anterior	79 (20.3)		<0.001*
Posterior	311 (79.7)		
Laterality			
Right Lung		4.74 ± 2.891	<0.001*
Left Lung		3.55 ± 2.05	
Lobar Distribution			
Right upper Lobe (RUL)		1.54 ± 1.112	
Right middle lobe (RML)		1.15 ± 0.987	
Right lower lobe (RLL)		2.06 ± 1.13	<0.001*
Left upper lobe (LUL)		1.53 ± 1.067	
Left lower lobe (LLL)		2.01 ± 1.128	

Citation: Parate R, Hundekari M, Anand A, Parate T, Ansari F. A Comprehensive Evaluation of High-Resolution Computed Tomography (HRCT) Imaging Patterns in COVID-19 Pneumonia According to the Time Course of the Disease and Across Different Age Groups in Indian Population. Indian J Appl Radiol. 2021;7(1): 162.

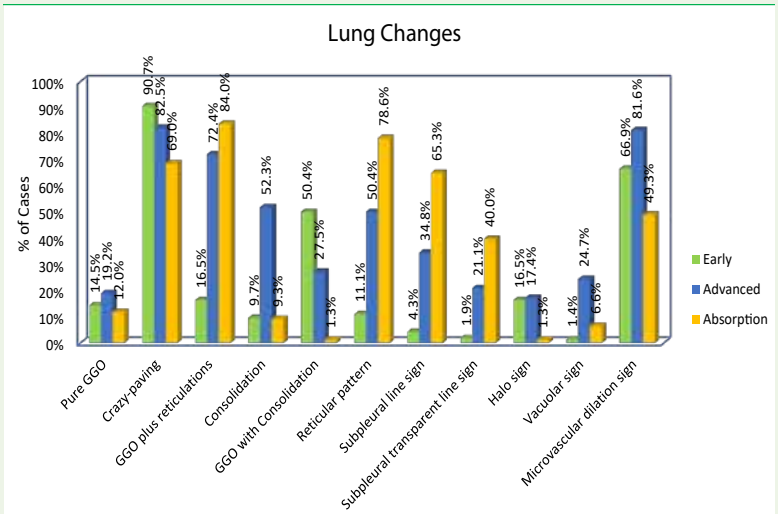

Figure 1: Bar graph shows the distribution of different HRCT patterns during the early (< 7 days), advanced (8-14 days) and absorption (> 14 days) phases of the disease.

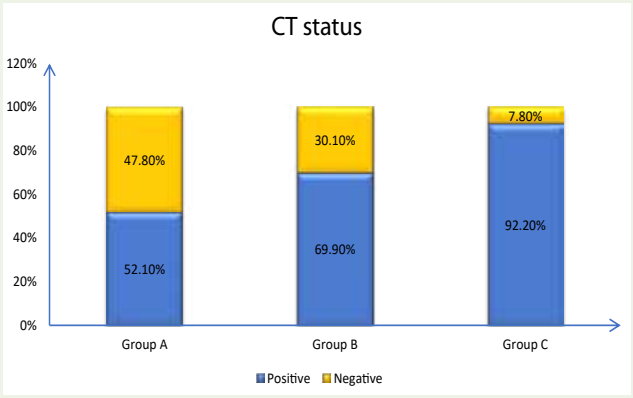

Figure 2: A stacked bar graph showing the percentage of positive and negative CT status among the different age groups. Group A (< 25 years), group B (25-44 years) and group C (≥ 25 years)

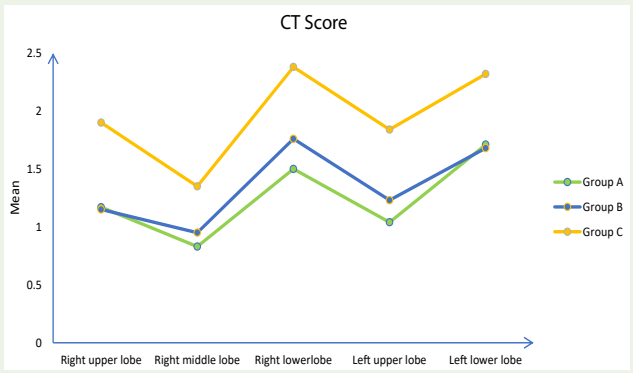

Figure 3: The line graph shows the Mean CT scores of each of the five lobes of the lung in different age groups.

Citation: Parate R, Hundekari M, Anand A, Parate T, Ansari F. A Comprehensive Evaluation of High-Resolution Computed Tomography (HRCT) Imaging Patterns in COVID-19 Pneumonia According to the Time Course of the Disease and Across Different Age Groups in Indian Population. Indian J Appl Radiol. 2021;7(1): 162.

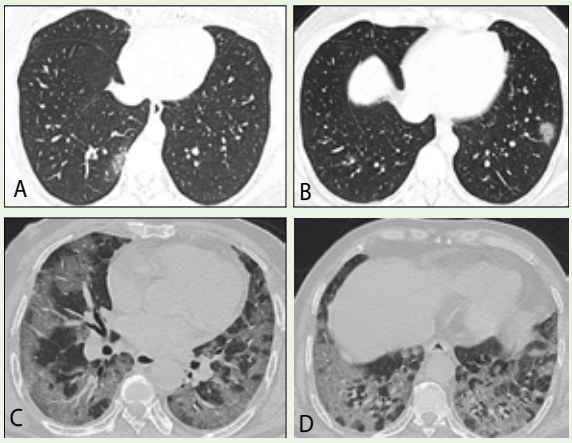

Figure 4: Distribution of lesion in 3 patients of different age groups with COVID-19 pneumonia. A, 25-year aged male. CT image obtained after 5 days of symptom onset shows a single lesion in the peripheral location that initially developed in the right lower lobe. B, 17-year aged female. CT image obtained after 3 days of symptom onset shows single lesion initially developed in the left lower lobe.C and D, 64-year aged male with CT image obtained 7 days after symptoms onset shows extensive bilateral distribution of crazy paving pattern.

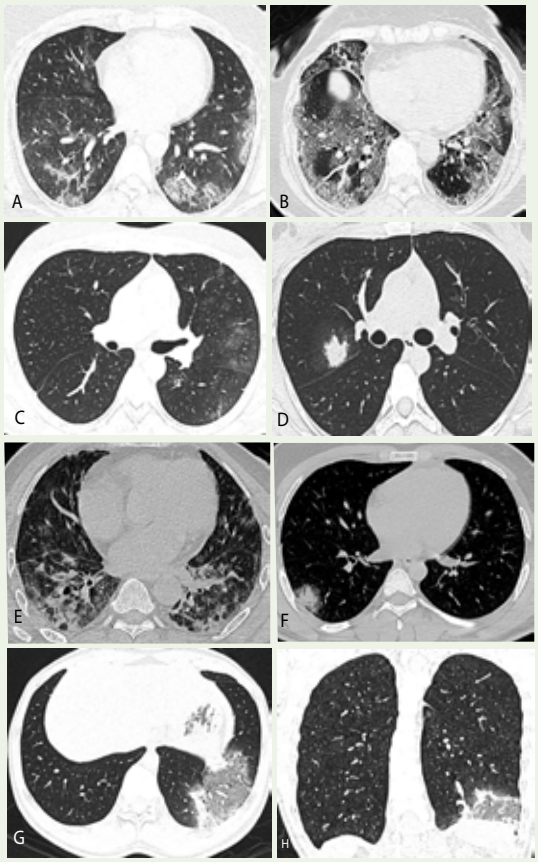

Figure 5: CT patterns observed in COVID-19 pneumonia. A, 30-year aged male showing GGO and GGO plus reticulations involving predominantly posterior area of the bilateral lower lobes. B, 46-year aged female showing crazy paving pattern- GGO along with interstitial thickening, the scan was obtained 8 days after symptom onset. C, 12-year aged male child with areas of pure GGO seen in left upper and lower lobes, the scan was done 4 days after onset of symptoms. D, 27-year aged female with consolidation noted in right middle lobe with the presence of air bronchogram within it. E, 50-year aged male showing GGO and GGO plus consolidation involving predominantly posterior area of the bilateral lower lobes. F, 26-year aged male showing Halo sign in right lower lobe, the scan was obtained9 days after symptom onset. G and H, 32-year aged male with areas of GGO surrounded by consolidation in left lower lobe- Reverse Halo sign.

Citation: Parate R, Hundekari M, Anand A, Parate T, Ansari F. A Comprehensive Evaluation of High-Resolution Computed Tomography (HRCT) Imaging Patterns in COVID-19 Pneumonia According to the Time Course of the Disease and Across Different Age Groups in Indian Population. Indian J Appl Radiol. 2021;7(1): 162.

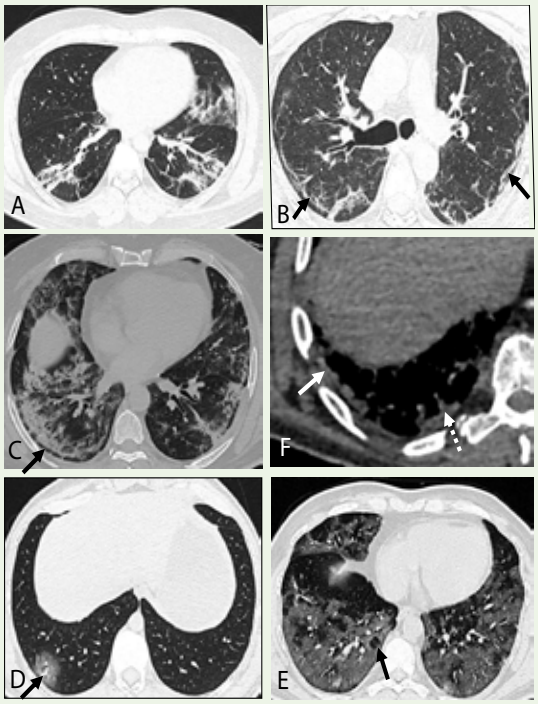

Figure 6: Other CT characteristics seen in COVID-19 pneumonia. A, 66-year aged male. CT image obtained after 15 days of symptom onset shows reticular streaks with bronchiectasis.B, 54-year aged female. CT image obtained after 18 days of symptom onset shows subpleural lines (arrows) in bilateral upper lobes. C, 32-year age male with CT image obtained 10 days after symptoms onset shows a subpleural transparent line (arrow). D, 20-year-old male shows microvascular dilation sign (arrow) in an area of ground-glass opacity. E, a 47-year-old male with extensive involvement of bilateral lower lobes, there are uninvolved areas of normal lung parenchyma seen scattered within (arrow)- Vacuolar sign. F, 52-year-old male: Pleural thickening (dotted arrow) and pleural retraction (solid arrow).

(264/390;67.7%) (Figure 2 and 3). Other patterns seen were Subpleural line sign (96/390;24.6%), Vacuolar sign (35/390;8.9%); Halo sign (54/390;13.8%) and Subpleural transparent line (57/390;14.6%). The patterns observed here are similar to those mentioned in previously conducted studies [9,10]. Some characteristics observed in our study were Reverse halo sign in 2/390 (<1%), cavitation in 4/390 (1%) and tree in bud appearance noted in 2/390 (<1%). Regarding bronchial changes, 64 patients (16.4%) showed air bronchogram sign and 37 patients (9.5%) showed bronchiectasis. The pleural changes noted were pleural thickening (78/390;20%), pleural retraction sign (60/390;15.3%) and pleural effusion (4/390;1%).

As per a preliminary COVID-9 pneumonia imaging diagnostic guide in China [11], we categorized the HRCT images into an early stage (≤ 7 days), advanced stage (8-14 days) and absorption stage (> 14 days) according to the disease course and compared each of the density characters among each phase (Table 4 and Figure 4). The predominant patterns in the early phase of the disease (≤ 7 days) were crazy-paving (187/206; 90.7%) and GGO with consolidation patterns (104/206; 50.4%) which were more common when compared to the absorption and advanced phases (P value<0.001). The consolidation pattern showed a significant increase during the advanced phase (57/109; 52.3%) as compared to the early phase (20/206;9.7%) (P-value < 0.001), furthermore, it decreased during the absorption phase (7/75;9.3%) (P-value < 0.001), however, no significant difference was seen between the early and absorption phase concerning this pattern (P-value=0.011). The vacuolar sign showed a significant rise during the advanced phase with a frequency of 27/82 (24.7%) when compared to the early and absorption phases (P-value<0.001). The GGO plus reticulations showed an increasing trend during the advanced and absorption phase as compared to early phase (P-value=<0.001 and 0.002 respectively). The reticular pattern, subpleural line sign and bronchiectasis showed increasing trends, highest frequency observed in the absorption phase (P-value<0.001). Not much difference was seen regarding the distribution of the following patterns: pure GGO (P=0.363), pleural thickening (P=0.615) and pleural retraction sign (P=0.742).

Furthermore, we compared the various parameters among the age groups as illustrated in Table 5. The positivity rate for abnormal scan for group B (165/236;69.9%) and C cases (201/218;92.2%) was significantly greater than the group A cases (24/46;52.1%) (P-value<0.001) (Figure 5). Overall, the mean CT score of each of the lung lobe was greatest in group C (P-value<0.001) (Figure 6). The total mean CT score was greater for group B and group C when compared to group A (F=22.550; P<0.001).

No significant difference was observed for the pure GGO and crazy-paving patterns among the age groups (P=0.483; P=0.126). The predominant patterns observed in group C were GGO plus

Citation: Parate R, Hundekari M, Anand A, Parate T, Ansari F. A Comprehensive Evaluation of High-Resolution Computed Tomography (HRCT) Imaging Patterns in COVID-19 Pneumonia According to the Time Course of the Disease and Across Different Age Groups in Indian Population. Indian J Appl Radiol. 2021;7(1): 162.

Table 3: HRCTimaging features of the patients with COVID-19 pneumonia.

Characteristics	Number (%) of patients (n = 390)
Single lesion	74 (18.9)
Multiple lesions	316 (81.1)
Size of the lesion	
< 1cm	38 (9.9)
1- 3 cm	53 (13.5)
≥ 3 cm	299 (76.6)
Lung change	
Pure GGO	60 (15.4)
Crazy- paving pattern	329 (84.4)
Consolidation	84 (21.5)
GGO with Consolidation	135 (34.6)
GGO plus Reticulations	176 (45.1)
Reticular pattern	137 (35.1)
Halo sign	54 (13.8)
Vacuolar sign	35 (8.9)
Microvascular dilatation sign	264 (67.7)
Subpleural line sign	96 (24.6)
Subpleural transparent line	57 (14.6)
Bronchial change	
Air bronchogram	64 (16.4)
Bronchiectasis	37 (9.5)
Pleural change	
Pleural thickening	78 (20)
Pleural retraction sign	60 (15.4)
Pleural effusion	4 (1)
Other findings	
Mediastinal lymphadenopathy	200 (51.3)
Calcification	78 (20)
Cavitation	4 (1)
Emphysematous changes	129 (33)
Tree in bud appearance	2 (0.5)

reticulations and reticular pattern, greater than the group A and group B cases (P<0.001). GGO with consolidation and consolidation patterns were more common in group B and C than in group A (P<0.001), without much difference, observed between group B and C (P>0.005). The relative representation of the following patterns: subpleural line sign, subpleural transparent line and vacuolar sign were more common in groups C as compared to group A and B (P<0.001). Further, no significant difference was observed for microvascular dilation sign (P=0.585), air bronchogram sign (P=0.384), bronchiectasis (P=0.617), pleural thickening (P=0.192), and the pleural retraction sign (P=0.106) among the age groups. Table 6 compares various HRCT patterns among different age groups.

Discussion

The COVID-19 pandemic has hit hard on the globe. Just as clinicians are evaluating more patients suspected of having the infection, radiologists are similarly interpreting more chest scans in those suspected of having COVID-19 pneumonia. It is also known that asymptomatic patients can have a positive chest HRCT with the converse also being true [12]. Moreover, considering the limited number of RT-PCR kits in some centres of the developing countries, with the added possibility of getting large false negative RT-PCR results, solely relying on the laboratory tests for confirmation of the diagnosiscould not be helpful. According to A rapid advance guide - Use of chest imaging in COVID-19, published by World Health Organization [WHO] [13], Chest imaging could be included as a part of the diagnostic workup of patients with suspected/probable COVID-19 infection in settings where the laboratory testing is not available or results are delayed or are initially negative in the presence of symptoms attributable to COVID-19. Moreover, the sensitivity of HRCT imaging is more as compared to the chest radiography as evaluated by some studies. In another literature review, the value and roles of different imaging modalities for the diagnosis and management of COVID-19, Chest radiography and HRCT scan were considered as key diagnostic modalities in suspected cases. With chest radiography having limited sensitivity for COVID-19 in the early stage of the disease, HRCT scan could be more accurate and sensitive in identifying pneumonia, especially during the early stages [14,15].

We conducted this retrospective study to study the spectrum of imaging characteristics. A positive HRCT rate was observed in a high proportion, 390/500 (78%) of RT-PCR confirmed symptomatic patients.

In a study conducted by Fang. Y et.al describing the CT image visual quantitative evaluation and clinical classification of COVID-19, 71.8 % symptomatic confirmed cases had CT evidence of pneumonia Zhan. J et.al reviewed CT scans of 110 patients describing CT pattern of evolution of COVID-19 pneumonia and reported an overall rate of 8.1 % negative scans [16,17]. Similarly, Liu. X et al. found a pooled positive CT rate of 89.7% cases among 2378 COVID-19 cases in a meta-analysis which included a total of 13 studies [18]. Thus, a comparable positive rate in this study could reflect the possible similar course of disease in Indian population as well as the fact that this study included only symptomatic positive patients; also 43.6% of cases belong to the age group ≥ 45 years. Some studies conducted in past have shown that the high proportion of elder age group (≥ 45 years) contributes towards a high positive rate [19].

We found higher mean CT score for right lung (4.74±2.89) than the left lung (3.55±2.05), with right lower lobe having highest mean score than the other lobes, a finding consistent with studies conducted previously [20]. The basis for this is, the bronchus of right lower lobe is more straighter, steep and is in continuation with the trachea. About 67.7% cases had a distribution of the lesions in the peripheral two-thirds of the lung and in 79.7% cases; posterior area of lungs was involved. The predominant patterns of lung opacities were crazy-paving pattern (84.4%), GGO with consolidation (34.6%) and GGO plus reticulations (45.1%), findings consistent with several studies as in a meta-analysis conducted by Bao et al. [18]. The microvascular dilation sign was accounted in 67.69 % cases. The various theories put forward regarding its etiology are disordered vasoregulation [21], pro-inflammatory cytokines induced vasodilation, alveolar-capillary microthrombi and infection-induced pulmonary vasculitis [22]. Lang et, al. even proposed that this disordered vasoregulation could be an early marker of ARDS onset even before the clinical symptoms and abnormal appearance on imaging [21].

When we compared the lung opacities among different phases,

Citation: Parate R, Hundekari M, Anand A, Parate T, Ansari F. A Comprehensive Evaluation of High-Resolution Computed Tomography (HRCT) Imaging Patterns in COVID-19 Pneumonia According to the Time Course of the Disease and Across Different Age Groups in Indian Population. Indian J Appl Radiol. 2021;7(1): 162.

Table 4: Comparison of HRCT patterns during different phases in 390 patients with COVID-19 pneumonia.

	EARLY PHASE	ADVANCED PHASE	ABSORPTION PHASE		
HRCT patterns	**No of patients (n=206)**	**No. of patients (n= 109)**	**No.of patients (n= 75)**	**Chi-Square Test Statistic**	**P-value**
Lung change					
Pure GGO	30 (14.5)[a]	21 (19.2)	9 (12)[b]	2.028	0.363
Crazy-paving	187 (90.7)[y]	90 (82.5)[y]	52 (69)[y]	19.528	<0.001*
GGO plus reticulations	34 (16.5)[a]	79 (72.4)[b]	63 (84)[x]	146.846	<0.001*
Consolidation	20 (9.7)[a]	57 (52.3)[b]	7 (9.3)[a]	84.678	<0.001*
GGO with Consolidation	104 (50.4)[y]	30 (27.5)[y]	1 (1.3)[y]	62.052	<0.001*
Reticular pattern	23 (11.1)[a]	55 (50.4)[b]	59 (78.6)[b]	125.538	<0.001*
Subpleural line sign	9 (4.3)[a]	38 (34.8)[b]	49 (65.3)[b]	118.685	<0.001*
Subpleural transparent line sign	4(1.9)[a]	23 (21.1)[b]	30 (40)[b]	68.915	<0.001*
Halo sign	34 (16.5)[b]	19 (17.4)[b]	1 (1.3)[a]	12.239	0.002*
Vacuolar sign	3 (1.4)[a]	27 (24.7)[b]	5 (6.6)[a]	48.036	<0.001*
Microvascular dilation sign	138 (66.9)[y]	89 (81.6)[y]	37 (49.3)[y]	21.317	<0.001*
Bronchial change					
Air Bronchogram sign	38 (18.4)[a]	26 (23.8)[a]	0[b]	19.749	<0.001*
Bronchiectasis	1 (0.4)[a]	15 (13.7)[b]	21 (28)[b]	51.692	<0.001*
Pleural change					
Pleural thickening	45 (21.8)[a]	19 (17.4)[b]	14 (18.6)[b]	0.971	0.615
Pleural retraction	29 (14.1)	18 (16.5)	13 (17.3)	0.596	0.742
Pleural effusion	0	4 (3.6)	0	10.419	0.005*

Note: * represents statistical difference among 3 groups; [a] and [b]show statistical significance; [x] does not show significant difference with other groups; [y] represents a significant difference with other groups

Table 5: Comparison of the extent of lung involvement among different age groups in patients with COVID-19 pneumonia

	Group A (< 25 years)		Group B (25 -44 years)		Group C (≥ 45years)			
	No.(%) of patients	**Mean ± SD**	**No.(%) of patients**	**Mean ± SD**	**No.(%) of patients**	**Mean ± SD**	**F value**	**P-value**
HRCT status								
Total	46		236		218	cc		
Positive	24 (52.1)		165 (69.9)		201 (92.2)			< 0.001*
Negative	22 (47.8)		71 (30.1)		17 (7.8)			
Laterality								
Right Lung		3.5 ± 2.75[a]		3.85 ±2.78[a]		5.62 ±2.72[b]	21.32	< 0.001*
Left Lung		2.75 ± 1.77[a]		2.91±2.0[a]		4.16 ±1.92[b]	20.842	< 0.001*
Lung lobe								
Right upper lobe		1.17 ±1.00[a]		1.15 ±1.08[a]		1.9 ±1.03[b]	24.29	< 0.001*
Right middle lobe		0.83 ± 0.9[x]		0.95±0.96[a]		1.35 ±0.97[b]	9.21	< 0.001*
Right lowerlobe		1.5 ± 1.10[a]		1.76 ±1.10[a]		2.38 ±1.06[b]	18.326	< 0.001*
Left upper lobe		1.04 ± 0.99[a]		1.23 ±1.01[a]		1.84 ±1.03[b]	19.179	< 0.001*
Left lower lobe		1.71 ± 0.9[x]		1.68 ±1.61[a]		2.32± 1.03[b]	17.023	< 0.001*
Total CT severity score		6.25 ± 4.37		6.76 ±4.65		9.79 ±4.48	22.55	< 0.001*

Note: * represents statistically significant difference; SD- Standard deviation;[a] and [b] show statistical significance; [x] does not show significant difference with other groups

we observed that during the early phase, the dominant patterns were crazy paving and GGO with consolidation. In early stages, the virus is likely to attack peripheral vessels and bronchi to cause an increase in the intraductal pressure which results in exudation, manifested as subpleural pure GGO. Over time, crazy-paving sign is formed due to thickening of the interlobular septum and increased exudation of the alveolus. If the disease continues to progress, the thickened lobular septum limits the absorption of the alveolar exudation, resulting in the alveolar consolidation formation. We observed that the consolidation, GGO plus reticulations and vacuolar sign were the predominant patterns in the advanced phase. Thus, the advanced phase could be described as a phase manifesting the combination of aggravation of the ongoing abnormalities along with initiation of repair changes within the parenchyma. This inhomogeneous

Citation: Parate R, Hundekari M, Anand A, Parate T, Ansari F. A Comprehensive Evaluation of High-Resolution Computed Tomography (HRCT) Imaging Patterns in COVID-19 Pneumonia According to the Time Course of the Disease and Across Different Age Groups in Indian Population. Indian J Appl Radiol. 2021;7(1): 162.

Table 6: Comparison of abnormal HRCT patterns among different age groups in patients with COVID-19 pneumonia.

	Group A (< 25 years)	Group B (25-44 years)	Group C (≥ 45 years		
HRCT findings	**No. (%) of patients (n=24)**	**No. (%) of patients (n=165)**	**No. (%) of patients (n=201)**	**Chi-Square Statistic**	**P-value**
Pure GGO	5 (20.8)[c]	28 (16.9)[d]	27 (13.4)[d]	1.454	0.483
Crazy- paving	17 (70.8)[c]	138 (83.6)[d]	174 (86.5)[d]	4.136	0.126
GGO with consolidation	11 (45.8)[c]	72 (43.6)[d]	52 (25.8)[d]	14.058	0.001*
Consolidation	2 (8.3)[c]	28 (16.9)[d]	54 (26.8)[d]	7.89	0.019*
GGO plus reticulation	3 (12.5)[z]	51 (30.9)[z]	122 (60.6)[z]	43.464	< 0.001*
Reticular pattern	3 (12.5)[z]	31 (18.7)[z]	103 (51.2)[z]	47.633	< 0.001*
Subpleural line sign	3 (12.5)[c]	17 (10.3)[c]	76 (37.8)[d]	38.794	< 0.001*
Subpleuraltransparent line sign	3 (12.5)[c]	9 (5.4)[c]	45 (22.3)[d]	20.913	< 0.001*
Air bronchogram	3 (12.5)[c]	32 (19.3)d	29 (14.4)[d]	1.914	0.384
Bronchiectasis	3 (12.5)[c]	13 (7.8)[w]	21 (10.4)[d]	0.967	0.617
Halo sign	6 (25)[c]	34 (20.6)[d]	14 (6.9)[w]	16.802	< 0.001*
Vacuolar sign	0[c]	7 (4.2)[c]	28 (13.9)[d]	12.932	0.002*
Microvascular dilation sign	17 (70.8)[c]	107 (64.8)[d]	140 (69.6)[d]	1.071	0.585
Pleural thickening	5 (20.8)[c]	26 (15.7)[d]	47 (23.3)[d]	3.304	0.192
Pleural retraction	5 (20.8)[c]	18 (10.9)[w]	37 (18.4)[d]	4.498	0.106
Pleural effusion	0[w]	2 (1.2)[w]	2 (0.9)[w]	0.307	0.858

Note: * represents statistical difference among 3 groups; [c] and [d]show statistical significance; [w]does not show significant difference with other groups; [z] represents a significant difference with all other groups.

involvement is evident by the vacuolar sign which is predominant during this phase. The absorption phase showed a predominance of the reticular pattern, subpleural line sign and subpleural transparent line sign which could be regarded as the repairing signs [10,23]. All the observed lesions could be eventually seen absorbing into irregular linear streaky opacities.

Furthermore, we noticed diversified patterns among different age groups of patients. Younger population < 25 years of age had a lesser extent of involvement than those above 45 years of age. This was supported by the fact that the mean total CT score of group C cases was significantly greater than group A cases. The patterns more commonly seen in elderly population included the GGO plus reticulations, reticular pattern, bronchiectasis and subpleural line sign. Deterioration of the lung structure and function along with a weaker immune system of the geriatrics could be the responsible factor for these patterns. Pleural thickening was mainly caused by the direct spread of the lesion, lymphatic reflux, and pleural inflammation. This may indicate that elderly patients show a more severe inflammatory response. At the same time, in elderly patients, whole lung lobes were more likely to be involved. This may indicate that in the same disease course, disease progression in elderly patients was faster than that in young patients [24,25].

Thus, our results fairly corroborate the distribution and types of pulmonary opacities reported in COVID-19 pneumonia worldwide. Also, the study findings are likely to help in understanding and evaluating the imaging abnormalities of cases during time course as well as depending upon the age and pattern of the patients. This could be a valuable tool in determining the treatment strategies as well as predicting prognosis of the disease. Therefore, it is essential to make full use of chest HRCT to achieve a comprehensive diagnosis and guide treatment for patients with COVID-19 infection.

But at the same time, it is pertinent to restrict the use of CT during the pandemic. Owing to the greater radiation dose of CT and the increased frequency of scans done presently, there is a growing concern regarding its long-term effects on the human body such as cancer, sterility, hematologic depression, etc. [26], thus it is of great importance to limit the number of scans done per person. Studies have shown that after the initial CT which is usually done after 5 days of symptom onset, appropriate follow-up time for subsequent chest scans should be during second week (approximately 12-14 days after symptoms onset) to look for disease progression and during fourth-fifth week to see for disease resolution [27]. Also, additional chest scans can be done when the patient shows acute exacerbation of the symptoms or deterioration and when the chest radiograph obtained is non-conclusive.

This study had many limitations. Firstly, only RT-PCR positive symptomatic cases were included in the study, this may have overruled the fact that many asymptomatic and RT-PCR negative yet infected cases were not evaluated which could have resulted in bias. Also, patterns like reticulations and bronchiectasis need further follow-up to note whether the fibrosis seen in COVID-19 is reversible or irreversible. Finally, no lung biopsies were performed to assess the correlation between radiological and histopathologic findings.

In summary, HRCT features of COVID-19 pneumonia vary according to the disease course and the patient's age. Crazy-paving pattern is dominant during the early phase and repairing signs during the absorption phase. The extent and pattern of involvement are more severe among the elderly population.

Acknowledgements

We express our gratitude to the Department of Radiology, Government Medical College Nagpur, Dr Ashwini Lahoti, Dr Pooja Raut and Dr Shivani Muppidwar for their support in providing necessary assistance in the recording of clinical and demographic data, and Mr Raghavendra Rao C. for helping in statistical analyses.

Citation: Parate R, Hundekari M, Anand A, Parate T, Ansari F. A Comprehensive Evaluation of High-Resolution Computed Tomography (HRCT) Imaging Patterns in COVID-19 Pneumonia According to the Time Course of the Disease and Across Different Age Groups in Indian Population. Indian J Appl Radiol. 2021;7(1): 162.

References

1. WHO Coronavirus Disease (COVID-19) Dashboard | WHO Coronavirus Disease (COVID-19).
2. Coronavirus India - live map tracker from Microsoft Bing.
3. Corman VM, Landt O, Kaiser M, Molenkamp R, Meijer A, Chu DK, et al. (2019) Detection of 2019 novel coronavirus (2019-nCoV) by real-time RT-PCR. Eurosurveillance 25: 2000045.
4. Ye G, Li Y, Lu M, Chen S, Luo Y, Wang S, et al. (2020) Experience of different upper respiratory tract sampling strategies for detection of COVID-19. J Hosp Infect 105: 1-2.
5. Xie X, Zhong Z, Zhao W, Zheng C, Wang F, et al. (2020) Chest CT for Typical Coronavirus Disease 2019 (COVID-19) Pneumonia: Relationship to Negative RT-PCR Testing. Radiology 296: 41-45.
6. Ai T, Yang Z, Hou H, Zhan C, Chen C, et al. (2020) Correlation of Chest CT and RT-PCR Testing for Coronavirus Disease 2019 (COVID-19) in China: A Report of 1014 Cases. Radiology 296: 32-40.
7. Salehi S, Abedi A, Balakrishnan S, Gholamrezanezhad A (2020) Coronavirus disease 2019 (COVID-19) imaging reporting and data system (COVID-RADS) and common lexicon: a proposal based on the imaging data of 37 studies. Eur Radiol 30: 4930-4942.
8. Francone M, Iafrate F, Masci GM, Coco S, Cilia F, et al. (2020) Chest CT score in COVID-19 patients: correlation with disease severity and short-term prognosis. Eur Radiol 30: 6808-6817.
9. Ding X, Xu J, Zhou J, Long Q (2020) Chest CT findings of COVID-19 pneumonia by duration of symptoms. Eur J Radiol 127: 109009.
10. Zhou S, Zhu T, Wang Y, Xia LM (2020) Imaging features and evolution on CT in 100 COVID-19 pneumonia patients in Wuhan, China. Eur Radiol 30: 5446–5454.
11. Chinese Clinical Guidance for COVID-19 Pneumonia Diagnosis and Treatment (7th edition)
12. Inui S, Fujikawa A, Jitsu M, Kunishima N, Watanabe S, Suzuki Y, et al.(2020) Chest CT Findings in Cases from the Cruise Ship Diamond Princess with Coronavirus Disease (COVID-19). Radiol Cardiothorac Imaging 2: 200110.
13. World Health Organization (2020) Use of chest imaging in COVID-19. 1–56.
14. Aljondi R, Alghamdi S (2020) Diagnostic Value of Imaging Modalities for COVID-19: Scoping Review. J Med Internet Res 22: 19673.
15. Borakati A, Perera A, Johnson J, Sood T (2020) Chest X-Ray Has Poor Sensitivity and Prognostic Significance in COVID-19: A Propensity Matched Database Study Author contribution (CRediT) statement.
16. Li K, Fang Y, Li W, Pan C, Qin P, Zhong Y, et al. (2020) CT image visual quantitative evaluation and clinical classification of coronavirus disease (COVID-19). Eur Radiol 30: 4407-4416.
17. Pan Y, Guan H (2020) Imaging changes in patients with 2019-nCov. Eur Radiol 30: 3612-3613.
18. Bao C, Liu X, Zhang H, Li Y, Liu J (2020) Coronavirus Disease 2019 (COVID-19) CT Findings: A Systematic Review and Meta-analysis. J Am Coll Radiol 17: 701–709.
19. Tabatabaei SMH, Talari H, Moghaddas F, Rajebi H (2020) CT Features and Short-term Prognosis of COVID-19 Pneumonia: A Single-Center Study from Kashan, Iran. Radiol Cardiothorac Imaging 2: 200130.
20. Zhou S, Wang Y, Zhu T, Xia L (2020) CT features of coronavirus disease 2019 (COVID-19) pneumonia in 62 patients in Wuhan, China. Am J Roentgenol 214: 1287-1294.
21. Lang M, Som A, Carey D, Reid N, Mendoza DP, et al. (2020) Pulmonary Vascular Manifestations of COVID-19 Pneumonia. Radiol Cardiothorac Imaging 2: e200277.
22. Ackermann M, Verleden SE, Kuehnel M, Haverich A, Welte T, et al.(2020) Pulmonary Vascular Endothelialitis, Thrombosis, and Angiogenesis in Covid-19. N Engl J Med 383: 120-128.
23. Wang Y, Dong C, Hu Y, Li C, Ren Q, Zhang X, et al.(2020) Temporal Changes of CT Findings in 90 Patients with COVID-19 Pneumonia: A Longitudinal Study. Radiology 296: 55-64.
24. Wang J, Zhu X, Xu Z, Yang G, Mao G, et al. (2020) Clinical and CT findings of COVID-19: differences among three age groups. BMC Infect Dis 20: 434.
25. Zhu T, Wang Y, Zhou S, Zhang N, Xia L (2020) A Comparative Study of Chest Computed Tomography Features in Young and Older Adults With Corona Virus Disease (COVID-19). J Thorac Imaging 35: 97-101.
26. Kalra MK, Maher MM, Rizzo S, Kanarek D, Shepard J-AO (2020) Radiation exposure from chest CT: issues and strategies. J Korean Med Sci 19: 159-166.
27. Chen C, Wang X, Dong J, Nie D, Chen Q, Yang F, et al. Temporal lung changes in high-resolution chest computed tomography for coronavirus disease 2019. J Int Med Res 48: 300060520950990.

Citation: Parate R, Hundekari M, Anand A, Parate T, Ansari F. A Comprehensive Evaluation of High-Resolution Computed Tomography (HRCT) Imaging Patterns in COVID-19 Pneumonia According to the Time Course of the Disease and Across Different Age Groups in Indian Population. Indian J Appl Radiol. 2021;7(1): 162.